13

Effects of B-site Donor and Acceptor Doping in Pb-free $(Bi_{0.5}Na_{0.5})TiO_3$ Ceramics

Yeon Soo Sung and Myong Ho Kim
Changwon National University
Korea

1. Introduction

$Pb(Zr,Ti)O_3$ (PZT)-based ceramics have been used extensively in various dielectric, piezoelectric, and ferroelectric applications because of their superior properties and versatility (Jaffe et al., 1971). The lead (Pb) content of PZT materials, however, poses serious problems for human health and the environment that can no longer be overlooked. It is inevitable that PZT will be replaced with Pb-free materials. PZT-based ceramics are still in use only because there are no materials that exhibit properties comparable to those of PZT.

The scientific community has intensively searched for and studied Pb-free piezoelectric materials. Among the few Pb-free materials available, solid solutions based on $(Bi_{0.5}Na_{0.5})TiO_3$ (BNT) (Isupov, 2005; Zhou et al., 2004; Park et al., 1996; Tu et al., 1994; Zvirgzds et al., 1982; Pronin et al., 1980; Jaffe et al., 1971) and $(Na_{0.5}K_{0.5})NbO_3$ (NKN) (Dai et al., 2009; Wang et al., 2007; Saito et al., 2004; Tennery & Hang, 1968; Haertling, 1967; Jaeger & Egerton, 1962; Egerton & Dillon, 1959) with a morphotropic phase boundary (MPB) have been considered as potential candidates for replacing PZT.

Each material has its merits and demerits. In terms of the piezoelectric coefficient (d_{33}), which is a key property, NKN-based ceramics appear to be the better choice considering their d_{33} of ~416 pC/N (Saito et al., 2004), which is high compared to the ~231 pC/N of BNT-based ceramics (Lin et al., 2006). However, NKN-based ceramics exhibit poor reproducibility because of hygroscopic problems. Furthermore, the range of temperature stability is narrow because those properties are mostly due to polymorphic phase transition. Regarding durability, BNT-based ceramics appear to be the better choice because, once sintered, they do not degrade as seriously as NKN-based ceramics do; this durability is an important factor in practical applications.

BNT has an ABO_3 perovskite structure with an A-site complex having rhombohedral symmetry at room temperature (Jaffe et al., 1971). It is known that BNT exhibits strong ferroelectricity with a high remnant polarization, coercive field, and conductivity. Because of its large coercive field and relatively high conductivity, BNT itself is difficult to pole, and consequently, its piezoelectric properties are not as appropriate for practical applications as those of PZT. As in the case of PZT, BNT-based solid solutions made with tetragonal $(Bi_{0.5}K_{0.5})TiO_3$ (BKT) or $BaTiO_3$ (BT) (Yu & Ye, 2008; Li et al., 2005; Kreisel et al., 2000; Takenaka et al., 1991) have been studied to improve the general properties by finding the MPB. MPB compositions of BNT-based binary, ternary, and complex solid solutions have

been found, but the properties obtained by the formation of the MPB are still inferior to those of PZT.

In improving the properties of solid solutions, the characteristics of end members should be thoroughly evaluated to understand the composition-dependent responses of solid solutions. However, there have been only a few reports on end member compounds; most of the studies have attempted to improve important material properties. The basic properties of BNT are not completely understood; unclear aspects remain. Regarding the understanding of BNT, there are reports on A-site modifications (Sung et al., 2010; Zuo et al., 2008; Kimura et al., 2005; Nagata et al., 2005), but there are only a few on B-site doping.

In this work, the effects of B-site doping in BNT ceramics were studied using a donor Nb^{5+} and an acceptor Mn^{3+} for B-site Ti^{4+}. Two key properties, dielectric depolarization temperature (T_d) and piezoelectric coefficient (d_{33}), were evaluated in relation to microstructure and phase purity. Then, they were compared with donor and acceptor effects in PZT (Jaffe et al., 1971; Zhang et al., 2008; Erhart et al., 2007; Zhang & Whatmore, 2003; Randall et al., 1998; Park & Chadi, 1998; Gerson, 1960) to identify similarities and differences between BNT and PZT ceramics. In addition, the electrical conductivity of BNT was measured and discussed as a function of the oxygen partial pressure and temperature.

2. Experimental

Powders of at least 3 N purity Bi_2O_3 (99.9%), Na_2CO_3 (99.95%), TiO_2 (99.9+%), Nb_2O_5 (99.9%), and Mn_2O_3 (99.999%) were used to prepare $(Bi_{0.5}Na_{0.5})(Ti_{1-x}D_x)O_3$ (D = Nb, Mn) ceramics through solid-state processing. In handling the raw powders, hygroscopic Na_2CO_3 was thoroughly dried in a dry-oven until no change in weight occurred. Then it was quickly weighed in air; if not, it absorbs moisture from the air and increases in weight, thus comprising an incorrect composition from the beginning.

The compositions of the samples were controlled to be x = 0–1 mol % for Nb doping and 0–2 mol % for Mn doping. The powders of each composition were ball-milled using yttria-stabilized zirconia balls and anhydrous ethanol to keep the powders from water. After milling, powders were dried and calcined twice at 780 °C and 800 °C for 2 h in air to prevent the premature loss of any component during calcination and to have homogeneous powders after calcination. Next, they were mixed with 5 wt% polyvinyl alcohol (PVA) aqueous solution to 0.5 wt% and screened using a 150 μm sieve for pelletizing. Pellets of 10 or 18 mm in diameter and ~1 mm in thickness were made by uniaxial pressing at 150 MPa. Then, all the samples were sintered at 1150 °C for 2 h in air. During sintering, the heating rate was controlled to burn out the PVA at around 500 °C.

The Archimedes principle was applied to estimate the apparent densities of the sintered pellets, and these values were compared with the theoretical densities. X-ray diffraction (XRD) patterns generated by a diffractometer with Cu Kα radiation (λ = 1.541838 Å) at 40 kV and 30 mA were taken from the polished surfaces of sintered pellets and analyzed for identifying phases. Scanning electron microscopy (SEM) with energy dispersive spectroscopy was used to detect any secondary phase formation as well as to examine grain morphology that occurred during sintering.

To measure their properties, the samples were polished on both sides down to 0.5 mm in thickness using #400, 800, and 1200 emery papers. They were painted with Ag paste and then cured at 650 °C for 0.5 h in air. Poling of samples was carried out at a dc field of 40

kV/cm for 0.5 h in silicone oil at room temperature using a high voltage supply (Keithley 248), and leakage current was monitored using an electrometer (Keithley 6514).
After aging for 24 h, the room temperature d_{33} was measured using a piezo d_{33} meter (ZJ-6B, IACAS) at 0.25 N and 110 Hz. The dielectric constant (ε) and the loss tangent (tan δ) at various frequencies on heating and cooling were measured using an impedance analyzer (HP4192A). The planar electromechanical coupling factors (k_p) and mechanical quality factors (Q_m) of the samples were calculated from the resonance frequencies (f_r), the antiresonance frequencies (f_a), the resonant impedances (Z_r), and the capacitances (C_p) at 1 kHz, measured using an impedance gain phase analyzer (HP4194A). Electric field dependent polarization (*P-E)* hysteresis loops were measured using a Sawyer-Tower circuit to measure remnant polarization (P_r) and coercive field (E_c).

3. Results

The weight losses of the samples that occurred during sintering were consistently less than 1 wt%. This was thought to primarily result from the evaporation of moisture, the PVA, and possibly some of the Bi and Na oxides. The relative apparent densities of the pellets after sintering were all above ~95% of the theoretical density, indicating that the samples were consistently prepared under the processing conditions used in this work.

3.1 Phase and microstructure

Figure 1 shows the XRD patterns of $(Bi_{0.5}Na_{0.5})(Ti_{1-x}D_x)O_3$ ceramics with D = Nb or Mn substituting for Ti in BNT. In the case of a donor Nb doping, no secondary peak was observed up to 1 mol %, and all the peaks were indexed to be rhombohedral. In the case of an acceptor Mn doping, XRD patterns were also phase-pure up to 2 mol %.

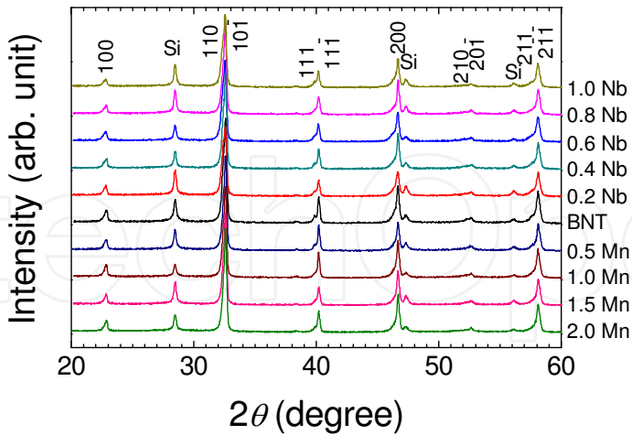

Fig. 1. XRD patterns of $(Bi_{0.5}Na_{0.5})(Ti_{1-x}D_x)O_3$ ceramics (D = Nb, Mn) sintered at 1150 °C for 2 h in air. Si peaks are of 5 N silicone powder used as an internal standard for calibration

The phase purity of the sintered $(Bi_{0.5}Na_{0.5})(Ti_{1-x}D_x)O_3$ with D = Nb or Mn pellets was confirmed by SEM images. No secondary phase was observed, as shown in Fig. 2. Regarding the grain morphology, the grain shapes in general were well developed in both

Nb and Mn doping, indicating that the sintering condition was consistent for both donor- and acceptor-doped samples.

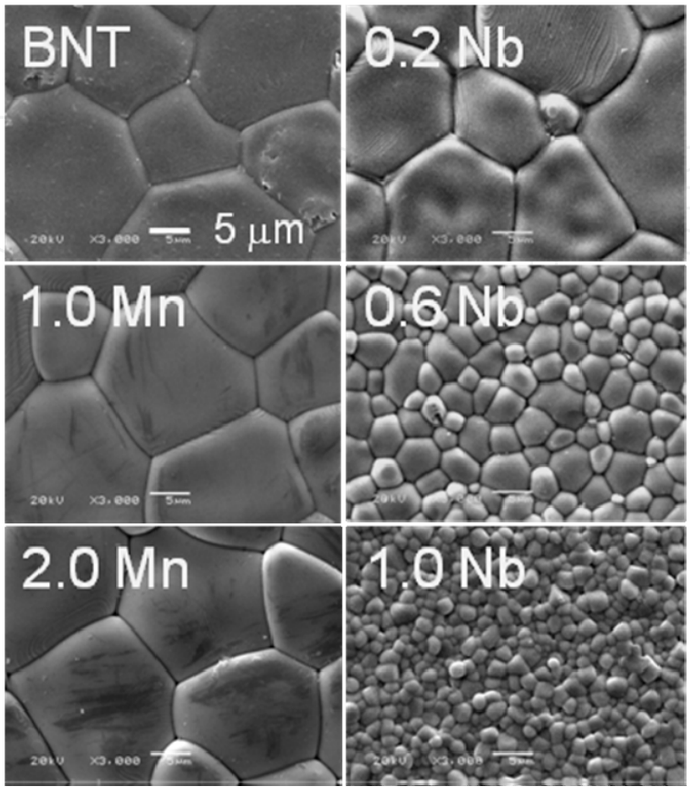

Fig. 2. SEM secondary electron images of the surfaces of $(Bi_{0.5}Na_{0.5})(Ti_{1-x}D_x)O_3$ pellets (D = Nb, Mn) sintered at 1150 °C for 2 h in air

An obvious difference observed among the images is the grain size relative to doping; the grain size decreased with Nb doping and increased with Mn doping, depending on the amount of Nb and Mn doping. The decrease in grain size in the case of Nb donor doping can be explained by A-site cation vacancies created by B-site donor doping required to maintain charge neutrality in the lattice. These cation vacancies exist along grain boundaries rather than inside grains, which is thermodynamically more stable. Grain boundaries would be pinned by these defects, inhibiting grain growth and resulting in relatively small grains in the case of donor doping (Yi et al., 2002; Lewis et al., 1985; Lucuta et al., 1985). Mn acceptor doping, on the other hand, induces oxygen vacancies instead of A-site vacancies required to maintain charge neutrality in the lattice. It appears that grain growth was not inhibited by Mn doping inducing oxygen vacancies, as shown in Fig. 2. These different roles of donor and acceptor that were observed in the microstructure affected the properties of BNT in different ways.

3.2 Piezoelectric properties

For various piezoelectric applications, d_{33}, k_p, and Q_m are key properties that need to be evaluated. As shown in Fig. 3, d_{33} gradually increased with Nb donor doping and gradually decreased with Mn acceptor doping. As mentioned above, B-site donor doping induces A-

site vacancy to maintain charge neutrality in the lattice. This A-site vacancy facilitates domain walls motion. Consequently, domains alignment during poling improves, resulting in a higher d_{33}.

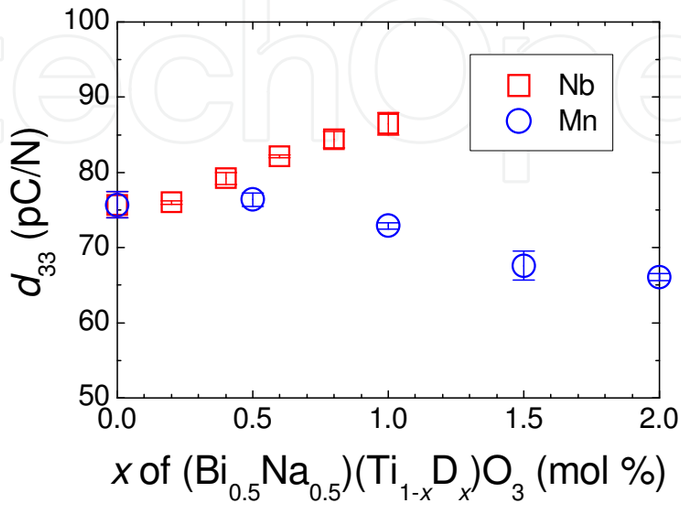

Fig. 3. Piezoelectric coefficient (d_{33}) of $(Bi_{0.5}Na_{0.5})(Ti_{1-x}D_x)O_3$ ceramics (D = Nb, Mn)

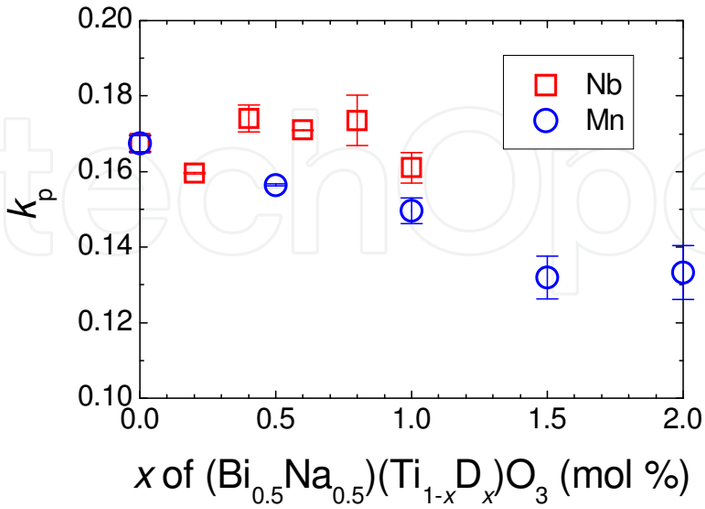

Fig. 4. Electromechanical coupling factor (k_p) of $(Bi_{0.5}Na_{0.5})(Ti_{1-x}D_x)O_3$ ceramics (D = Nb, Mn)

B-site acceptor doping, on the other hand, reduces A-site vacancy or induces oxygen vacancy to maintain charge neutrality in the lattice. Acceptor doping produces the results that are opposite to those produced by donor doping, as shown in Fig. 3. Oxygen vacancy is relatively mobile; this pins domain walls (Zhang & Whatmore, 2003; Park & Chadi, 1998), resulting in a lower d_{33} unless the vacancy becomes immobile by forming defect complexes with other defects (Hu et al., 2008; Zhang et al., 2008; Erhart et al. 2007). The increase from donor doping and the decrease from acceptor doping in the d_{33} of BNT ceramics are generally consistent with the variations from doping in the d_{33} of PZT-based ceramics (Jaffe et al., 1971). Regarding the microstructure, d_{33} appears to be inversely related to grain size.
The trend observed in k_p, as shown in Fig. 4, was similar to that observed in d_{33}. A slight increase from Nb donor doping and a gradual decrease from Mn acceptor doping occurred; this is consistent with the typical outcomes of B-site donor and acceptor doping in PZT.

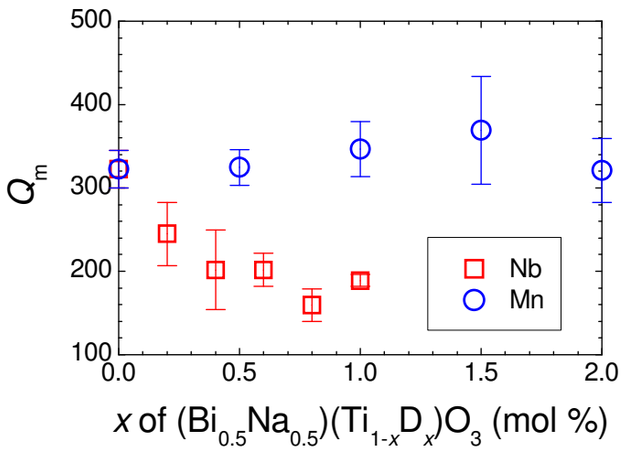

Fig. 5. Mechanical quality factor (Q_m) of $(Bi_{0.5}Na_{0.5})(Ti_{1-x}D_x)O_3$ ceramics (D = Nb, Mn)

Q_m, on the contrary, decreased with Nb donor doping and increased with Mn acceptor doping, as shown in Fig. 5. Regarding mechanical loss, it is expected that the grain boundary would cause more loss than the grain itself. As grain size increases, grain boundary area decreases, yielding a higher Q_m. This result can be coupled with the variation in grain size according to doping, as shown in Fig. 2. Q_m became smaller as grain size became smaller with Nb donor doping, but it became slightly larger as grain size became slightly larger with Mn acceptor doping.

3.3 Dielectric properties

For measuring dielectric properties according to changes in doping, the samples were pre-poled to expose T_d, as indicated by the arrow marks in Fig. 6. With Nb donor doping both room temperature ε and tan δ increased while with Mn acceptor doping, ε did not change significantly and tan δ decreased, as shown in Fig. 6. These dielectric results of BNT with B-site donor and acceptor doping are similar to those of PZT with doping, although the two are dielectrically different materials.

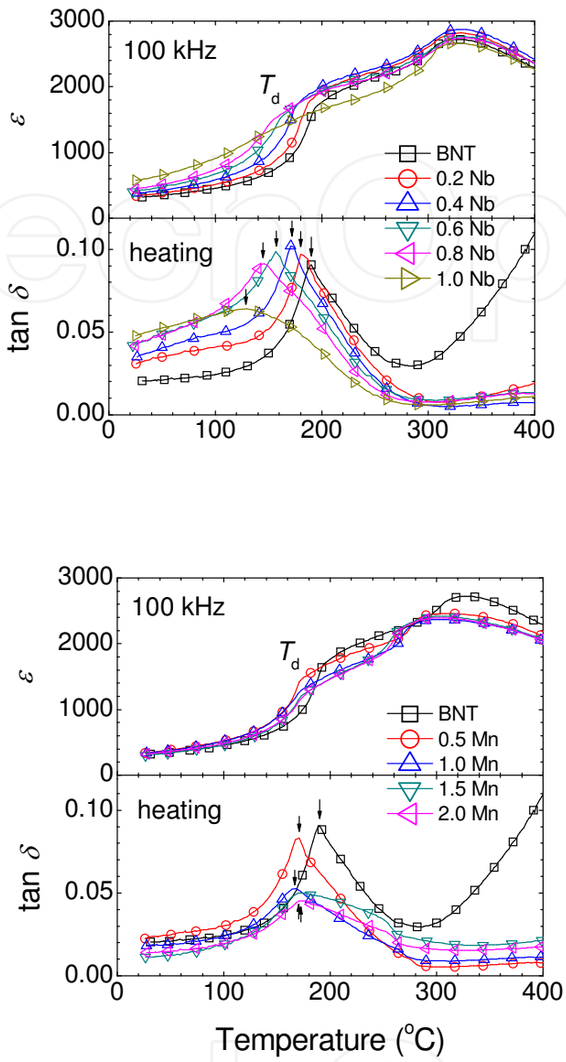

Fig. 6. Dielectric constant (ε) and loss tangent (tan δ) of $(Bi_{0.5}Na_{0.5})(Ti_{1-x}D_x)O_3$ ceramics (D = Nb, Mn). Arrow marks indicate the depolarization temperature (T_d)

Two transitions appeared; the temperature maximum (T_m) at ε maximum (ε_m) and T_d. In the case of Nb donor doping, T_m did not change significantly and T_d decreased gradually, as shown in Fig. 6. In the case of Mn acceptor doping, both T_{max} and T_d decreased to 0.5 mol % then did not change significantly with further Mn doping, as shown in Fig. 6. The variations in T_d of BNT ceramics with donor and acceptor doping are shown in Fig. 7.

BNT is dielectrically different from PZT. As a relaxor exhibiting frequency dependence and a broad transition, BNT is dielectrically lossy because of the to space-charge contribution (Hong & Park, 1996). A polymorphic phase transition occurs as lattice symmetry changes from rhombohedral to tetragonal, then to cubic symmetry. In addition, BNT has a unique transition, T_d, unlike PZT. For practical applications, this T_d of ~200 °C is considered to be a critical drawback of BNT because its temperature stability is lower than that of PZT.

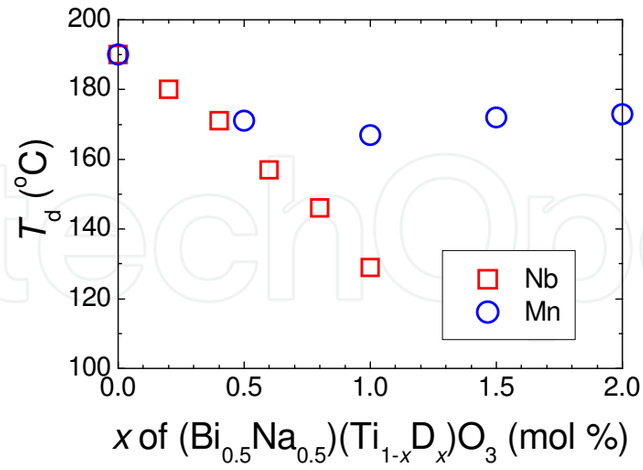

Fig. 7. Depolarization temperature (T_d) of $(Bi_{0.5}Na_{0.5})(Ti_{1-x}D_x)O_3$ ceramics (D = Nb, Mn)

3.4 Electrical properties

In oder to determine the electrical conductivity of BNT ceramics, the resistivity of the sample was measured as a function of temperature (T) and oxygen partial pressure (pO_2), then converted into electrical conductivity (σ).

The sample was attached to Pt wires (ϕ = 0.2 mm) according to the four probe method to eliminate the non-ohmic contact. The low oxygen pressure was established using an O_2/Ar mixture. Figure 8 shows σ of BNT ceramics in the range of T = 700–900 °C and $pO_2 = 10^0$–10^{-5} atm.

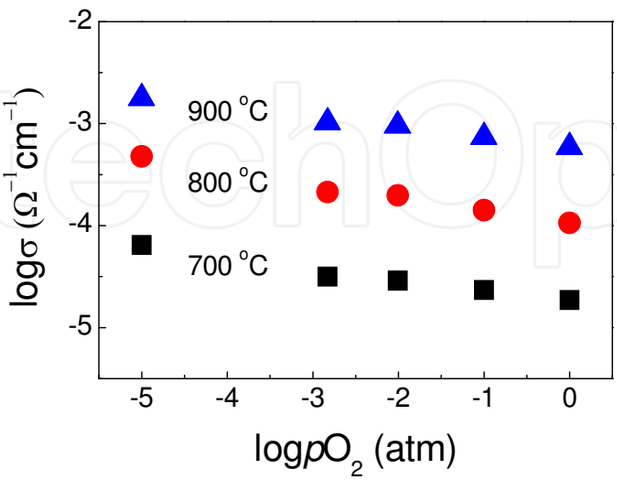

Fig. 8. Electrical conductivity (σ) of BNT ceramics as a function of oxygen partial pressure (pO_2) at 700, 800, and 900 °C

In the experimental results, the $d\log\sigma/d\log pO_2$ slopes are clearly negative in the temperature range tested. Therefore, the conduction behavior of BNT can be considered as *n*-type in the elevated temperature range.

3.5 Other properties

In addition to the above-mentioned piezoelectric and dielectric properties, other properties, such as ferroelectric and electrical properties, must be considered in relation to practical applications. For instance, E_c, P_r, and leakage current density (J_{leak}) are important properties that need to be characterized. Table 1 summarizes certain properties measured with various B-site donors and acceptors.

As shown in Table 1, with donor doping, E_c decreased and P_r increased. Similar results were obtained regardless of the donor material (Nb^{5+}, Ta^{5+}, or W^{6+}). With acceptor doping, on the other hand, E_c increased and P_r decreased. Overall, there were consistent trends in the case of donors, but the results with acceptors were not as consistent as those with donors.

Regarding J_{leak} at room temperature, there were some difficulties in taking the measurement; J_{leak} was very low at zero field and was only ~10^{-8} A/cm² at a dc poling field of 40 kV/cm. There were no consistent and reliable data values in the literature to compare because of differences among samples that were caused by different sample preparation methods.

	BNT	donor			acceptor	
	Ti^{4+}	Nb^{5+}	*Ta^{5+}	†W^{6+}	Mn^{3+}	Sc^{3+}
ionic radius (Å)	0.605	0.64	0.64	0.60	0.645	0.745
phase purity (mol %)	yes	1.0	0.8	0.4	2.0	0.8
grain size (μm)	~20	~2	~5	~5	>20	~15
d_{33} (pC/N)	74	87	84	84	66	77
k_p	0.17	0.17	-	0.16	0.13	0.16
Q_m	320	160	202	180	369	269
ε	324	↑	-	↑	-	-
tan δ	0.02	↑	-	-	↓	↑
T_d (°C)	190	129	-	-	167	-
E_c @ 60 Hz (kV/cm)	*~41	*~24	~18	~20	-	-
P_r @ 60 Hz (μC/cm²)	*~35	-	-	~40	-	-
J_{leak} @ 40 kV/cm (A/cm²)	~10^{-8}	-	-	-	-	-

Table 1. Effects of various B-site donors and acceptors in $(Bi_{0.5}Na_{0.5})(Ti_{1-x}D_x)O_3$ ceramics. The ionic radius of Ti^{4+} is given for BNT in comparison with donors and acceptors at coordination number 6 (Shannon, 1976). The values for phase purity are not the solubility limits of doping but merely indicate the phase purity confirmed experimentally up to that point. The variation in the values for BNT is thought to be mostly due to differences in sample preparation. *(Yeo et al., 2009) and †(Cho et al., 2008)

4. Discussion

PZT has been studied for decades and its properties have been categorized in detail, while only a few reports and studies are available for BNT. The effects of donor and acceptor doping on both BNT and PZT ceramics are summarized in Table 2. The trends related to

donor and acceptor doping observed in BNT ceramics are similar to those observed in PZT, but there are also some differences.

For ABO_3 perovskite, as mentioned above, B-site donor doping induces A-site vacancies while acceptor doping reduces A-site vacancies and induces oxygen vacancies to maintain charge neutrality in the lattice. A-site vacancies facilitate domain walls motion (Gerson, 1960), which explains a high d_{33} and dielectric loss (Jaffe et al, 1971). Oxygen vacancies, on the other hand, are mobile and pin domain walls; this restricts domain switching, resulting in a low d_{33} and dielectric loss. Oxygen vacancies, however, can be tied up with cation vacancies forming defect complexes that make them immobile (Hu et al., 2008; Zhang et al., 2008; Erhart et al. 2007; Zhang & Whatmore, 2003; Park & Chadi, 1998). If this occurs, domain walls motion is not hindered but grain growth is hindered by grain boundary pinning caused by defect complexes (Sung et al., 2010).

Coupling the piezoelectric values with the microstructural variations in Fig. 2, a higher d_{33} was obtained from smaller grains with Nb donor doping, and a lower d_{33} was obtained from larger grains with Mn acceptor doping. This implies that, in the case of Nb donor doping, the domain walls must have been unpinned, leading to a high d_{33}, while grain boundaries must have been pinned, causing small grains. The situation was reversed in the case of Mn acceptor doping. Domain walls must have been pinned, leading to a low d_{33}, while grain boundaries must have been unpinned, causing large grains. This indicates that oxygen vacancies, if they were formed by Mn acceptor doping must have been tied up by the formation of defect complexes.

	donor		acceptor	
	‡PZT	BNT	‡PZT	BNT
d_{33}	↑	↑	↓	↓
k_p	↑	-	↓	↓
Q_m	↓	↓	↑	↑
ε	↑	↑	↓	-
tan δ	↑	↑	↓	↓
T_c or T_d	-	↓	-	↓
E_c	↓	↓	↑	-
P_r	-	↑	-	-
J_{leak}	↓	-	↑	-

Table 2. Comparison of the effects of donor and acceptor doping in BNT ceramics (given in Table 1) with those in PZT ceramics ‡(Jaffe et al., 1971). For acceptor doping effects, Mn was counted, but Sc was not

Two key properties involved in the practical application of BNT-based ceramics are d_{33} and T_d. T_d especially is a limiting factor because the piezoelectric properties of BNT-based ceramics diminish above T_d. For improved temperature stability, therefore, it is important to have a higher T_d. However, d_{33} has exhibited an inverse relationship with T_d. In other words, as T_d increases, d_{33} decreases, and vice versa (Sung et al., 2010). This is similar to the relationship between d_{33} and Curie temperature (T_c) in $PbTiO_3$, as d_{33} increases, T_c decreases, and vice versa.

With acceptor doping, both d_{33} and T_d decreased then remained constant. With donor doping, on the other hand, these two properties exhibited an inverse relationship. This inverse relationship was observed in Bi-based titanate end members as well as their solid

solutions, but it has not been clearly explained, partly because T_d is a unique transition in BNT-based ceramics that cannot be explained in terms of the PZT database. Sung et al. suggested lattice distortion as a common factor that affects the two properties inversely. If lattice distortion decreases, d_{33} increases through better poling by electric field, but T_d decreases through easier depoling by temperature.

For doping effects in general, all the explanations have been given in terms of A-site and oxygen-site vacancies. In terms of the ionic sizes, Mn^{3+}, Ti^{4+}, Nb^{5+}, Ta^{5+}, and W^{6+} (but not Sc^{3+}) are similar, as shown in the comparison with Ti^{4+} in Table 1. In cases of similar ionic size, there will be minimal change in the shape and size of the lattice. With a small amount of doping, therefore, it would be difficult to detect any variation in the XRD patterns. Indeed, as shown in Fig. 9, there was no apparent change in peak positions caused by Nb donor or Mn acceptor doping. It would be interesting to know if any variation in lattice parameters occurs in the case of a substantial amount of doping with a relatively large difference in ionic radii.

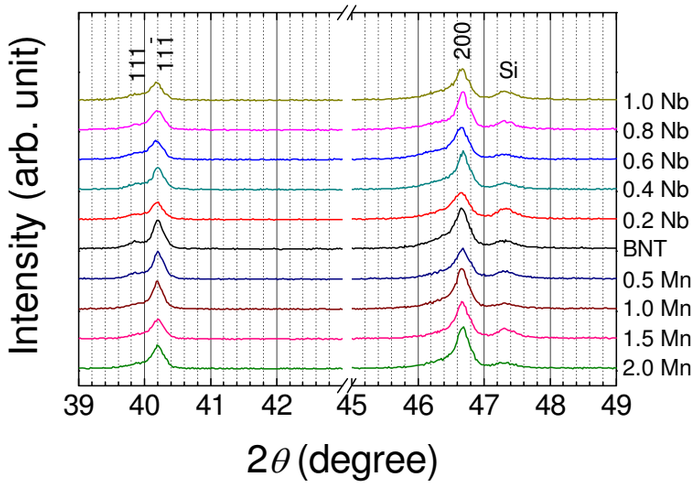

Fig. 9. Detailed XRD patterns of $(Bi_{0.5}Na_{0.5})(Ti_{1-x}D_x)O_3$ ceramics (D = Nb, Mn), from the patterns shown in Fig. 1

There are some data regarding donor doping effects in BNT-based ceramics, but little information is available about acceptor doping effects. This situation could exist because acceptors with 3+ valence can be on either the B-site Ti or the A-site vacancy, considering the volatile A-site Bi^{3+} and Na^{1+}. For dornors with 5+ or 6+, on the other hand, it is unlikely that they would occupy the A-site vacancy instead of the B-site Ti. Moreover, even if they did, the resulting outcomes would still be considered as donor doping effects. As shown in Table 2, among the data on donor effects, consistent trends can be identified. Grain size, Q_m, T_d, and E_c decreased, while d_{33} and P_r increased. These trends become reversed with acceptor doping.

Finally, it cannot be emphasized enough that hygroscopic Na_2CO_3 must be completely dried before and during weighing. Otherwise, the nominal compositions of the samples will be

incorrect. If the ionic radius of an acceptor with 3+ valence is larger than that of Ti^{4+}, doping of an acceptor with 3+ valence on Na^{1+} vacancy, instead of the Ti^{4+} site, might occur. In addition, there is the possibility of an acceptor with 3+ valence substituting for A-site Bi^{3+} instead of for B-site Ti^{4+}. This appears to explain the inconsistent results and donor-like effects (see Table 1) that were observed in Sc^{3+}, which has a larger ionic radius than the others do as compared with that of Ti^{4+}. To confirm the acceptor effects in BNT, the next experiment should include the doping of acceptors with 2+ valence and small differences in ionic radii.

5. Summary

The effects of a B-site donor, Nb^{5+}, and an acceptor, Mn^{3+}, for Ti^{4+} in Pb-free $(Bi_{0.5}Na_{0.5})(Ti_{1-x}D_x)O_3$ (D = Nb or Mn) ceramics were studied in terms of microstructure and important properties. Regarding the microstructure, all the samples retained a perovskite structure with rhombohedral symmetry with both Nb donor and Mn acceptor doping. No secondary phase was seen up to x = 1.0 mol % of Nb-doped BNT ceramics and x = 2.0 mol % of Mn-doped BNT ceramics. The grain size, however, decreased with Nb doping and slightly increased with Mn doping. In addition to producing variation in microstructure, Nb and Mn yielded opposite piezoelectric and dielectric outcomes. Higher d_{33}, lower Q_m, and smaller grain size were obtained from Nb doping, while lower d_{33}, higher Q_m, and larger grain size were obtained from Mn doping. These results indicate a correlation between piezoelectric properties and grain size. Regarding the dielectric transition, T_d decreased with Nb doping, but it decreased slightly then held steady with Mn doping. Overall, the donor effects observed in BNT ceramics were similar to those observed in PZT ceramics, but acceptor effects need to be studied further in order to produce consistent data. At elevated temperatures, BNT exhibited n-type conduction.

6. Acknowledgments

This work was supported by the National Research Foundation of Korea Grant funded by the Korean Government (2009-0088570) and the Basic Science Research Program through the National Research Foundation of Korea (NRF) funded by the Ministry of Education, Science and Technology (2010-0025055). This research was also financially supported by the Ministry of Education, Science and Technology (MEST) and Korea Institute for Advancement of Technology (KIAT) through the Human Resource Training Project for Regional Innovation.

7. References

Cho, J. H.; Yeo, H. G.; Sung, Y. S.; Song, T. K.; & Kim, M. H. (2008). Dielectric and piezoelectric characteristics of W-doped lead-free $(Bi_{0.5}Na_{0.5})(Ti_{1-x}W_x)O_3$ ceramics. *New Physics: Sae Mulli* (The Korean Physical Society) 57, 409-416.

Dai, Y. J.; Zhang, X. W.; Chen, K. P.; (2009). Morphotropic phase boundary and electrical properties of $K_{1-x}Na_xNbO_3$ lead-free ceramics. *Appl. Phys. Lett.*, 94, 042905.

Egerton, L. & Dillon, D. M. (1959). Piezoelectric and dielectric properties of ceramics in the system potassium-sodium niobate. *J. Am. Ceram. Soc.*, 42, 438-442.

Erhart, P.; Eichel, R.; Traskelin, P. & Albe, K. (2007). Association of oxygen vacancies with impurity metal ions in lead titanate. *Phys. Rev. B*, 76, 174116.

Gerson, R. (1960). Variation in ferroelectric characteristics of lead zirconate titanate ceramics due to minor chemical modifications. *J. Appl. Phys.*, 31, 188-194.

Haertling, G. H. (1967). Properties of hot-pressed ferroelectric alkali niobate ceramics. *J. Am. Ceram. Soc.*, 50, 329-330.

Hong, K. S. & Park, S. E. 1996. Phase relations in the system of ($Na_{1/2}Bi_{1/2}$)TiO_3-$PbTiO_3$. II. Dielectric property. *J. Appl. Phys.*, 79, 388-392.

Hu, G. D.; Fan, S. H.; Yang, C. H. & Wu, W. B. (2008). Low leakage current and enhanced ferroelectric properties of Ti and Zn codoped $BiFeO_3$ thin film. *Appl. Phys. Lett.*, 92, 192905.

Isupov, V. A. (2005). Ferroelectric $Na_{0.5}Bi_{0.5}TiO_3$ and $K_{0.5}Bi_{0.5}TiO_3$ perovskites and their solid solutions. *Ferroelectrics*, 315, 123-147.

Jaeger, R. E. & Egerton, L. (1962). Hot pressing of potassium-sodium niobates. *J. Am. Ceram. Soc.*, 45, 209-213.

Jaffe, B.; Cook, Jr. W. R.; & Jaffe, H. (1971). *Piezoelectric Ceramics*, Academic Press, New York. ISBN 0-12-379550-8.

Kimura, T.; Fukuchi, E. & Tani, T. (2005). Fabrication of textured bismuth sodium titanate using excess bismuth oxide. *Jpn. J. Appl. Phys.*, 44, 8055-8061.

Kreisel, J.; Glazer, A. M.; Jones, G.; Thomas, P.; Abello, L. & Lucazeau, G. (2000). An x-ray diffraction and Raman spectroscopy investigation of A-site substituted perovskite compounds: the $(Na_{1-x}K_x)_{0.5}Bi_{0.5}TiO_3$ ($0 \le x \le 1$) solid solution. *J. Phys. Condens. Mat.*, 12, 3267-3280.

Lewis, G. V.; Catlow, R. A. & Casselton, R. E. W. (1985). PTCT effect in $BaTiO_3$. *J. Am. Ceram. Soc.*, 68, 555-558.

Li, Y.; Chen, W.; Zhou, J.; Xu, Q.; Sun, H. & Liao, M. (2005). Dielectric and ferroelectric properties of lead-free $Na_{0.5}Bi_{0.5}TiO_3$-$K_{0.5}Bi_{0.5}TiO_3$ ferroelectric ceramics. *Ceram. Int.*, 31, 139-142.

Lin, D.; Xiao, D.; Zhu, J. & Yu, P. (2006). Piezoelectric and ferroelectric properties of $[Bi_{0.5}(Na_{1-y}K_xLi_y)_{0.5}]TiO_3$ lead-free piezoelectric ceramics. *Appl. Phys. Lett.*, 88, 062901.

Lucuta, P. GR.; Constantinescu, FL. & Barb, D. (1985). Structural dependence on sintering temperature of lead zirconate-titanate solid solutions. *J. Am. Ceram. Soc.*, 68, 533-537.

Nagata, H.; Shinya, T.; Hiruma, Y.; Takenaka, T.; Sakaguchi, I. & Haneda, H. (2005). Piezoelectric properties of bismuth sodium titanate ceramics. *Ceram. Trans.* 167, 213-221. ISBN 978-1-57498-188-9.

Park, C. H. & Chadi, D. J. (1998). Microscopic stud of oxygen-vacancy defects in ferroelectric perovskites. *Phys. Rev. B*, 57, R13961-R13964.

Park, S. E.; Chung, S. J.; Kim, I. T. (1996). Ferroic phase transitions in ($Na_{1/2}Bi_{1/2}$)TiO_3 crystals. *J. Am. Ceram. Soc.*, 79, 1290-1296.

Pronin, I. P. ; Syrnikov, P. P.; Isupov, V. A.; Egorov, V. M. & Zaitseva, N. V. (1980). Peculiarities of phase transitions in sodium-bismuth titanate. *Ferroelectrics*, 25, 395-397.

Randall, C. A.; Kim, N.; Kucera, J.; Cao, W. & Shrout, T. R. (1998). Intrinsic and extrinsic size effects in fine-grained morphotropic-phase-boundary lead zirconate titanate ceramics. *J. Am. Ceram. Soc.*, 81, 677-688.

Saito, Y.; Taka, H.; Tani, T.; Nonoyama, T.; Takatori, K.; Homma, T.; Nagaya, T. & Nakamura M. (2004). Lead-free piezoceramics. *Nature*, 432, 84-87.

Shannon, R. D. 1976. Revised effective ionic radii and systematic studies of interatomic distances in halides and chalcogenides. *Acta Cryst*. A32, 751-767.

Sung, Y. S.; Kim, J. M.; Cho, J. H.; Song, T. K.; Kim, M. H.; Chong, H. H.; Park, T. G.; Do, D. & Kim, S. S. (2010). Effects of Na nonstoichiometry in $(Bi_{0.5}Na_{0.5+x})TiO_3$ ceramics. *Appl. Phys. Lett.*, 96, 022901.

Sung, Y. S.; Kim, J. M.; Cho, J. H.; Song, T. K.; Kim, M. H.; Park, T. G. (2010). Roles of lattice distortion in $(1-x)(Bi_{0.5}Na_{0.5})TiO_3$-$xBaTiO_3$ ceramics. *Appl. Phys. Lett.*, 96, 202901.

Takenaka, T.; Maruyama, K. & Sakata, K. (1991). $(Bi_{1/2}Na_{1/2})TiO_3$-$BaTiO_3$ system for lead-free piezoelectric ceramics. *Jpn. J. Appl. Phys.*, 30, 2236-2239.

Tennery, V. J. & Hang, K. W. (1968). Thermal and X-ray diffraction studies of the $NaNbO_3$-$KNbO_3$ system. *J. Appl. Phys.*, 39, 4749-4753.

Tu, C. S.; Siny, I. G. & Schmidt, V. H. (1994). Sequence of dielectric anomalies and high-temperature relaxation behavior in $Na_{1/2}Bi_{1/2}TiO_3$. *Phys. Rev. B*, 49, 11550-11559.

Wang, Y.; Damjanovic, D.; Klein, N.; Hollenstein, E. & Setter, N. (2007). Compositional inhomogeneity in Li- and Ta-modified $(K,Na)NbO_3$ ceramics. *J. Am. Ceram. Soc.*, 90, 3485-3489.

Yeo, H. G.; Sung, Y. S.; Song, T. K.; Cho, J. H.; Kim, M. H. & Park, T. G. (2009). Donor doping effects on the ferroelectric and the piezoelectric properties of Pb-free $(Bi_{0.5}Na_{0.5})TiO_3$ ceramics. *J. Korean. Phys. Soc.*, 54, 896-900.

Yi, J. Y.; Lee, J. K. & Hong, K. S. (2002). Dependence of the microstructure and the electrical properties of lanthanum-substituted $(Na_{1/2}Bi_{1/2})TiO_3$ on cation vacancies. *J. Am. Ceram. Soc.*, 85, 3004-3010.

Yu, H. & Ye, Z. G. (2008). Dielectric, ferroelectric, and piezoelectric properties of the lead-free $(1-x)(Na_{0.5}Bi_{0.5})TiO_3$-$xBiAlO_3$ solid solution. *Appl. Phys. Lett.*, 93, 112902.

Zhou, Z. H.; Xue, J. M.; Li, W. Z.; Wang, J.; Zhu, H. & Miao, J. M. (2004). Ferroelectric and electrical behavior of $(Na_{0.5}Bi_{0.5})TiO_3$ thin films. *Appl. Phys. Lett.*, 85, 804-806.

Zvirgzds, J. A. ; Kapostins, P. P.; Zvirgzde, J. V. & Kruzina, T. V. (1982). X-ray study of phase transitions in ferroelectric $Na_{0.5}Bi_{0.5}TiO_3$. *Ferroelectrics*, 40, 75-77.

Zuo, R.; Su, S.; Wu, Y.; Fu, J.; Wang, M. & Li, L. (2008). Influence of A-site nonstoichiometry on sintering, microstructure and electrical properties of $(Bi_{0.5}Na_{0.5})TiO_3$ ceramics. *Mater. Chem. Phys.*, 110, 311-315.

Zhang, Z.; Wu, P.; Lu, L. & Shu, C. (2008). Defect and electronic structures of acceptor substituted lead titanate. *Appl. Phys. Lett.*, 92, 112909.

Zhang Q. & Whatmore, R. W. (2003). Improved ferroelectric and pyroelectric properties in Mn-doped lead zirconate titanate thin films. *J. Appl. Phys.*, 94, 5228-5233.

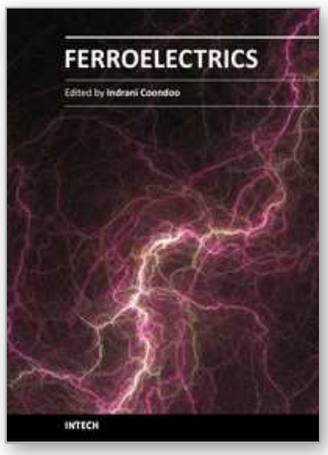

Ferroelectrics

Edited by Dr Indrani Coondoo

ISBN 978-953-307-439-9
Hard cover, 450 pages
Publisher InTech
Published online 14, December, 2010
Published in print edition December, 2010

Ferroelectric materials exhibit a wide spectrum of functional properties, including switchable polarization, piezoelectricity, high non-linear optical activity, pyroelectricity, and non-linear dielectric behaviour. These properties are crucial for application in electronic devices such as sensors, microactuators, infrared detectors, microwave phase filters and, non-volatile memories. This unique combination of properties of ferroelectric materials has attracted researchers and engineers for a long time. This book reviews a wide range of diverse topics related to the phenomenon of ferroelectricity (in the bulk as well as thin film form) and provides a forum for scientists, engineers, and students working in this field. The present book containing 24 chapters is a result of contributions of experts from international scientific community working in different aspects of ferroelectricity related to experimental and theoretical work aimed at the understanding of ferroelectricity and their utilization in devices. It provides an up-to-date insightful coverage to the recent advances in the synthesis, characterization, functional properties and potential device applications in specialized areas.

InTech Europe
University Campus STeP Ri
Slavka Krautzeka 83/A
51000 Rijeka, Croatia
Phone: +385 (51) 770 447
Fax: +385 (51) 686 166
www.intechopen.com

InTech China
Unit 405, Office Block, Hotel Equatorial Shanghai
No.65, Yan An Road (West), Shanghai, 200040, China
中国上海市延安西路65号上海国际贵都大饭店办公楼405单元
Phone: +86-21-62489820
Fax: +86-21-62489821

IntechOpen